

## Original Research Article

# Green synthesis of $\text{CoFe}_2\text{O}_4$ ferrofluid: Investigation of structural, magnetic and rheological behaviour

Meet A. Moradiya\*<sup>ORCID</sup>, Pradeep Kumar Khiriya<sup>ORCID</sup>, Purnima Swarup Khare

School of Nanotechnology, Rajiv Gandhi Proudyogiki Vishwavidyalaya, Bhopal, Madhya Pradesh, India

### ARTICLE INFORMATION

Received: 8 May 2021

Received in revised: 5 June 2021

Accepted: 7 June 2021

Available online: 24 July 2021

DOI: 10.26655/AJNANOMAT.2021.3.9

### KEYWORDS

Green synthesis

Cobalt ferrite

Ferrofluid

Rheology

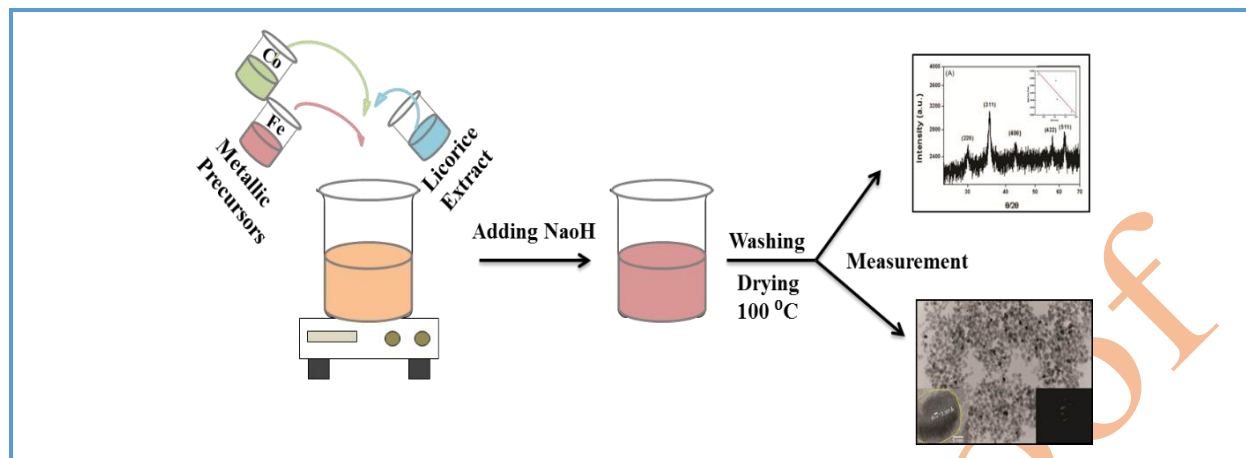
Magnetization

### ABSTRACT

In this work, we report the green synthesis of cobalt ferrite ( $\text{CoFe}_2\text{O}_4$ ) nanoparticles Ferrofluid by a modified co-precipitation method using *Glycyrrhiza glabra* (Licorice) roots as a surfactant, which is eco-friendly, non-toxic, and inexpensive. X-Ray diffraction (XRD) analysis confirmed the purity of the spinel  $\text{CoFe}_2\text{O}_4$  structure. The average crystallite size, strain and lattice constant were 5 nm, 0.01, and  $8.39 \text{ \AA}$ , respectively. Fourier transform infrared spectrum (FTIR) results demonstrated an absorption band at a wavenumber of  $574 \text{ cm}^{-1}$ , indicating the presence of cobalt ferrite nanoparticles. transmission electron microscopy (TEM) images showed that the sample contains well-dispersed and spherical nanoparticles with an average particle size of 12.6 nm. The magnetic properties of the fluid are confirmed from the (M-H) hysteresis curve. The hysteresis curve revealed the ferromagnetic nature of the particles, and the saturation magnetization ( $M_s$ ) is  $56.6 \text{ emu/g}$ . The rheological properties were studied with a variable magnetic field rheometer. The results showed that the rheological measurements comply with the structural and magnetic properties of the CFO FF by a green modified co-precipitation synthesis *G. glabra*, which can be used for various medical applications.

© 2021 by SPC (Sami Publishing Company), Asian Journal of Nanoscience and Materials, Reproduction is permitted for noncommercial purposes.

## Graphical Abstract



## Introduction

Ferrofluids (FF), also called magnetic fluids, are colloidal solutions of magnetic nanoparticles in a fluid carrier such as water and organic solvents (i.e. Kerosene) [1–3]. Ferrofluid (FF) has unique physical, chemical, and biocompatible properties [4–6]. Cobalt ferrite ( $\text{CoFe}_2\text{O}_4$ ) is a well-known magnetic material with a high coercivity ( $H_c$ ) and moderate magnetization ( $M_s$ ). These properties, along with their excellent physical and chemical stability, make  $\text{CoFe}_2\text{O}_4$  (CFO) nanoparticles suitable for various medicinal and biological applications, as well as for phase separation, elimination of pollutants from water, and sensing [7–12]. There are various methods of synthesis CFO nanoparticle such as microwave, double sintering, hydrothermal, citrate complex, thermal decomposition, auto combustion, micro-emulsion, sol-gel processing, and mechanochemical [13, 23].

The goal of today is to develop those synthesis approaches for nanomaterials that are eco-friendly, simple, and reduce the use of hazardous substances chemical products [14–17]. The best synthesis approach is the combination of the methods of soft chemistry and green chemistry. The best option of soft

chemistry technique of synthesis is the co-precipitation method. The co-precipitation method has various advantages such as high yield, high purity, less use of organic solvents, and low cost [18]. Various researchers have proposed green chemistry methods to prepare the nanomaterials [19–21]. Numerous surfactants and reducing agents can be used to synthesize nanomaterials, such as oleic acid, sodium borohydride, CTAB, Polyvinyl alcohol, plant extracts etc. [14]. They used to control the size and agglomerations of nanomaterials. In addition, the plant extract which is naturally available and less costly than other surfactant and reducing agents [22–24]. The *G. glabra* (Licorice) roots extract controls the existing surface energy of the particle so that the surface tension decreases, allowing more particles to escape the aggregation process and generally lowering the particle size of as-prepared CFO FF. Thus the CFO FF obtained through green approaches could be used in various medical applications, including radio frequency hyperthermia, magnetic drug delivery and magnetic resonance imaging.

Ferrites are magnetic oxide particles that are very stable under normal conditions over a long period. Ferrites are a group of oxide compounds with the formula of  $\text{AB}_2\text{O}_4$ , where A and B are

divalent and trivalent ions, respectively. Magnetic colloidal fluids are complex fluids that show a significant change in their rheological properties under an external magnetic field [13]. These fluids express non-Newtonian effects in the existence of the magnetic field. Therefore, it is magnetically induced rheological properties help develop magnetofluidic devices. The cobalt ferrite ( $\text{CoFe}_2\text{O}_4$ ) is interesting because of its high magnetocrystalline anisotropy, high coercivity, and moderate magnetic saturation [14]. Recently, various plant extracts such as leaves, flowers, fruits, and roots, are used to obtain metal oxides and mixed metal-oxide nanoparticles [25–33]. A literature review showed that the root extract of *Glycyrrhiza glabra* was often used to obtain Au and Ag nanoparticles [34]. In 2015, Manikandan and his research colleagues reported the first study on copper ferrite ( $\text{CuFe}_2\text{O}_4$ ) preparation using *Hibiscus rosa-sinensis* extract [35]. Dana Gingasu *et al.* demonstrated the preparation of  $\text{CoFe}_2\text{O}_4$  nanoparticles by self-combustion in which the ginger/cardamom extracts act as a reducing agent [36]. K. Kombaiah *et al.* developed the green method for synthesizing cobalt ferrite nanoparticles using Okra (*A. esculentus*) plant extract as a reducing agent [37].

To the best knowledge of the author, although the root extract of *Glycyrrhiza glabra* has been used to prepare Au and Ag nanoparticles [34], its use for the synthesis of CFO FF has not been reported so far. *G. glabra* root (Licorice) is considered as one of the oldest and most used herbs around the world [38]. Licorice is conventionally used in herbal medicines for its emollient, demulcent, and gastroprotective properties [39]. *G. glabra* has a wide range of activities such as antioxidant, anti-helicobacterpyloric, estrogen-like activity, anti-nephritic, and radical scavenging activities

[40]. Several bioactive compounds in *G. glabra* have been reported, including glycyrrhizic acid, saponin, glycyrrhizin, and glucuronic acid [41]. This work deals with the green preparation and optimization of the  $\text{CoFe}_2\text{O}_4$  nanoparticles in relevance to Ferrofluid using *G. glabra* as a surfactant. The optimization of the size and characterization of nanoparticles was carried out using XRD, TEM, VSM, and magnetorheometer. The rheological properties by varying shear rate and magnetic field have been studied in detail.

## Experimental

### Materials and methods

The chemical reagents required for the synthesis are Cobalt (II) Chloride ( $\text{CoCl}_2$ ), Iron (III) Chloride ( $\text{FeCl}_3$ ), Sodium Hydroxide ( $\text{NaOH}$ ), Kerosene as a carrier fluid, DD water and Ethanol. All the chemical reagents were bought from Sigma-Aldrich chemicals. The extract was prepared in the laboratory using *Glycyrrhiza glabra* roots.

### Preparation of *Glycyrrhiza glabra* root extract

The root of *Glycyrrhiza glabra* was collected from the local surroundings of the Bhopal region, India and were authenticated by Dr. Hardik Soni from Vasu Research Centre, Vadodara, India (voucher number SN/080312). About 10 g of *G. glabra* roots were grounded into a fine powder and extracted for 1.5 h in 100 mL of water at 80 °C. After boiling, the collected extract was filtered using the Whatman 42 filter paper and then centrifuged at 8000 rpm for 15 min to remove undissolved particulates. The collected extract was stored at 4 °C for nanoparticles synthesis. This *Glycyrrhiza glabra* root extract acts as a surfactant. The compound present in the extract of *G. glabra* extract can include various combinations of organic and

inorganic reducing agents, and in particular, the saponins have extraordinary surfactant properties [23, 24].

#### *Synthesis of $\text{CoFe}_2\text{O}_4$ Ferrofluid (CFO FF)*

The environmental friendly CFO FF was formed by a modified co-precipitation technique, using Cobalt (II) Chloride and Iron (III) Chloride salt solution. 0.4 M (25 mL) solution of iron chloride and 0.2 M (25 mL) of cobalt chloride solutions were mixed in double distilled (DD) water. After that, the 20 mL of *G. glabra* roots extract was added with continuous stirring at 80 °C for 45 min on a magnetic stirrer. DD water was used as a solvent to avoid the formation of contaminations in the final product. A 2 M (25 mL) solution of sodium hydroxide (NaOH) was prepared and added slowly to the salt solution dropwise (9 mL/min). The pH of the solution was constantly monitored when adding the NaOH solution. The mixed chemical reactants were constantly stirred using a magnetic stirrer until a pH of 11-12 was reached. The magnet verified the stability of the fluid. A stable colloidal did not stabilize by a strong magnetic field which led to the formation of CFO FF capped with the help of saponin. The precipitate was then brought to a reaction temperature of 70 °C and stirred for 1 h. The prepared product was then cooled to room temperature. The semi-solid precipitate was washed twice with DD water and then with Ethanol to remove the sodium and chlorine compounds, as well as the surfactant from the solution. To separate the supernatant liquid, the beaker contents were then centrifuged for 15 min at 3500 rpm. The supernatant liquid was transfer to the centrifugation machine until only thick black precipitate remained. The precipitate was then dried overnight at 100 °C. Then the dried precipitate was ground and calcined at 600 °C for 6 h. These particles are directly dissolved in a carrier fluid (Kerosene)

to get Ferrofluid. The particles are mixed in the Kerosene using continuous stirring under normal heating to obtain a homogeneous colloid of CFO FF. The fluid obtained is stable against the gravitational and magnetic field for a very long duration of time.

#### *Characterization of $\text{CoFe}_2\text{O}_4$ based Ferrofluid*

The X-ray diffraction (XRD) patterns of the samples were recorded on the Rikagu Ultima IV multiple X-ray diffractometer (MXRD) is used for the structural investigation of particles. The data were collected in the angular range from 20° to 60° in steps of 0.02° with 1 s scan time per step. Copper  $\text{K}\alpha$ , having a wavelength ( $\lambda_{\text{Cu-K}\alpha}$ ) 0.154056 nm used to generate X-rays by heating a filament operating at 40 kV and 30 mA. The monochromatic beam from the Copper source achieved using a 0.5% Nickel filter ( $\text{K}\beta$ -filter). The instrument has a horizontal goniometer with theta/2theta geometry having a 570 mm diameter. The particle shape, size distribution, and microstructure were analyzed using the TEM (Tecnai G2 F30 S-TWIN). A vibrating sample magnetometer (VSM) is the most appropriate instrument to measure the magnetization of the magnetic fluid as a function of the magnetic field. Lake Shore VSM is used to study the room temperature magnetic measurements. It can measure magnetic moments ranging from  $10^{-7}$  emu to  $10^3$  emu. The magnetoviscous properties of Ferrofluid were investigated with a Rheometer (Anton Paar MCR301) equipped with an external controllable magnetic field.

## **Results and Discussion**

### *Structural and Microscopic Properties*

Figure 1a shows the X-ray diffraction pattern of cobalt ferrite nanoparticles. The characteristics peaks of spinel ferrite with

preferred orientation along (220), (311), (400), (422), and (511) planes (JCPDS card no. : 22-1086.). All the peaks in the pattern correspond to the single-phase cubic spinel structure (space group  $Fd\bar{3}m$ ), and the absence of any other peak confirms the purity of the sample. The broad diffraction peaks indicate the presence of ultrafine nature of particles. The crystallite size (D) for the samples is calculated by using Scherrer formula  $D = K\lambda/\beta\cos\theta$ , where K is Scherrer's constant (0.89), for X-ray wavelength ( $=1.54056\text{\AA}$ , for Cu  $K_{\alpha}$  target),  $\beta$  is FWHM (Full Width at Half Maxima) of the corresponding diffraction peak measured in radians and  $\theta$  is the angle between the sample surface and the diffracted beam [42]. The average size of the crystallites determined from the width of the X-ray diffraction lines using the Debye Scherrer formula has been estimated to be approximately 5 nm. The lattice constant of the Ferrofluid is found to be  $a=8.39\text{\AA}$ . The strain ( $\epsilon$ ) was found to be  $\sim 0.01$  from the Williamson-Hall (W-H) method, which is shown in the inset of Figure 1a. Fourier Transform Infrared Spectroscopy (FTIR) spectroscopy is a helpful tool for identifying the functional groups of any organic molecule. The FTIR spectrum of CFO FF is shown in Figure 1b. The appearance of a peak at  $574\text{ cm}^{-1}$  is attributed to the absorption of metal oxide (M-O), which indicates cobalt ferrite nanoparticles [43]. The peaks at around  $1050$ ,  $1400$ ,  $1574$ ,  $2850$ , and  $2925\text{ cm}^{-1}$  are due to O-H bending vibrations, C-O bending, C-H bending, C-H stretching, and O-H stretching, respectively [44]. Figure 1c shows the TEM image of the as-prepared Ferrofluid. Spherical morphology of particles observed from the image. The diameter of the particles measured from images is plotted as a histogram shown in Figure 1d. The HRTEM image confirms the crystalline nature of the magnetic nanoparticles shows in the inset of Figure 1c. The SAED patterns demonstrate the

well-developed lattice fringes of as-prepared CFO FF, which is shown in the inset of Figure 1c. Figure 1d depicts the histogram of as-synthesized Ferrofluid plotted to form the graphs with different magnifications show that the particle size is about 12.6 nm on average.

### *Magnetic and rheological properties*

Figure 2a demonstrates the effect of an applied magnetic field on the magnetization (emu/g) value of prepared cobalt ferrite ferrofluid at room temperature. The M-H curves of as-prepared CFO FF indicate hysteresis loop formation for magnetic materials with high coercivity,  $H_c \sim 2003$ . It was also observed that by increasing the strength of the applied field, the value of the saturation magnetization ( $M_s$ ) for as-synthesized material sharply increases and becomes nearly saturated at about  $56.6\text{ (emu/g)}$ , suggesting the presence of small magnetic particles exhibiting ferromagnetic nature of CFO FF [36]. Figure 2b depicts the effect of varying magnetic fields (0 to 1 T) on the viscosity of CFO FF was evaluated by applying constant shear of  $50\text{ s}^{-1}$ . It is observed that by increasing the field intensity, the viscosity of the Ferrofluid is also increased. This is because of the dipole-dipole intrinsic interactions constructing a chain-like complex network that aligns with the the applied magnetic field. With the increase of the field, the dipole interactions become significant, which enhances the viscosity of as-prepared Ferrofluid [45]. The dipole moment of a magnetic particle is directly proportional to its volume of a magnetic core with the relation given by  $\mu = V\chi H$ , where  $V = \pi d^3/6$  is the volume of the particle,  $d$  is the diameter of the particle,  $\chi$  is the magnetic susceptibility of the particle and  $H$  is the applied magnetic field [45]. It can also be seen that the increase in the field beyond 0.8 T leads to saturation in the as-prepared sample due to saturation of the dispersed

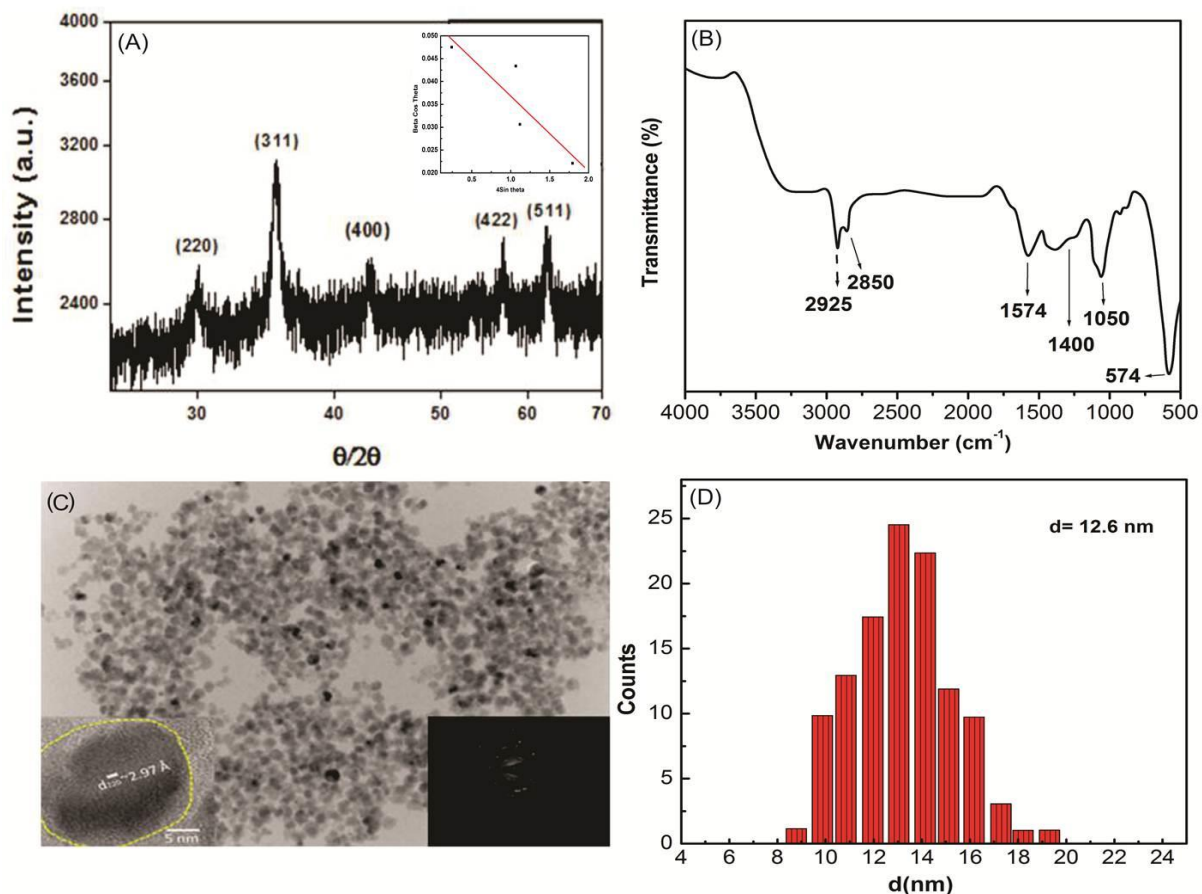


**Figure 1.** a) XRD patterns for the CFO FF; inset shows the Williamson Hall (W-H) Plot of as-prepared material, b) FTIR spectra of as-synthesized CFO FF, c) TEM image of  $\text{CoFe}_2\text{O}_4$  FF; inset shows the HRTEM and SAED patterns of as-prepared Ferrofluid, d) Histogram of CFO FF

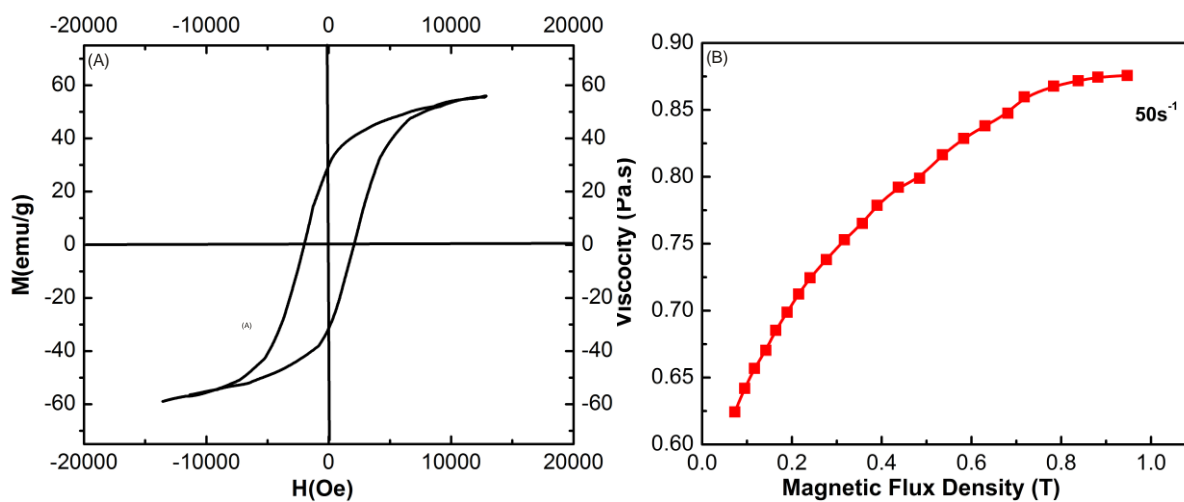


**Figure 2.** a) Hysteresis loop of as-prepared Ferrofluid, b) Magneto viscous effects of  $\text{CoFe}_2\text{O}_4$  Ferrofluid

magnetic particles and agglomerated size. Furthermore, the viscosity decreases with a decrease in the density of the number of particles because of weak dipolar interaction.

The shear stress for the as-prepared sample was plotted against the variable shear rate, which is shown in [Figure 3a](#); as the shear rate increases, the shear stress continues to increase. This makes the Ferrofluid to offer more resistance to the disc rotation with increased shear rates. The highest value of shear stress is  $\sim 177$  Pa. It is interesting to note that the rheology of CFO FF is very sensitive to the size of the particles in the presence of a magnetic field. The Bingham model, then the others, can better describe the rheological behaviour of ferrofluid samples because the curve shows a larger linear region. The dynamic yield stress of magneto-rheological fluids is calculated according to the plastic model of Bingham [46]. The rheological properties of CFO FF were studied on the MCR301 Rheometer at room temperature. The inset of [Figure 3a](#) shows the shear dependent viscosity for all samples in the presence of an applied magnetic field (0.95 T). The viscosity of the sample is higher at the low shear rate, but when it increases the shear rate (25–250/s), it decreases from 12.03 to 1.02 mPas. This demonstrates a shear thinning behaviour at the narrow limit and the Newtonian behaviour for a wide range of shear rates. It is attributed to the fact that the lower shear rate cannot break the magnetically induced structures, but as the shear rate increases, these structures break, and fluid flows easily. Therefore, the viscosity of the Ferrofluid decreases quickly with an increase in the shear rate. To evaluate the effect of the number density of the particles, a time-dependent viscosity measurement was performed. [Figure 3b](#) shows the time-dependent viscosity versus time of CFO FF at a constant shear rate. In this [Figure 3b](#), the three

regions can be considered as a region (I) without magnetic field, region (II) with a magnetic field, and region (III) without a magnetic field. The abrupt increase in viscosity at the boundary regions I and II shows the rapid formation of magnetic structures. This may be due to the increase in dipole-dipole interaction, leading to the formation of chain-like clusters and ultimately to the improvement of viscosity. When the magnetic field is cancelled, the viscosity is faced with a sudden drop and destroys the chain-like structures. However, it is remarkable to note that the viscosity in region III is higher than the initial viscosity in the region I. This means that part of the structures formed has not been destroyed, or new aggregates have been restored. The decrease in viscosity over time in region III is linked to a progressive distortion of the aggregate structures, indicating larger particles in the sample [47].

The strain amplitude sweep of as-prepared CFO FF is done to study the variation in the elastic property (storage modulus,  $G'$ ) and the viscous property (loss modulus,  $G''$ ) by applying a varying strain amplitude (0-100%) at the constant field (0.5 T) and constant angular frequency ( $\omega = 50$  rad/sec), [Figure 4a](#). The data sets were mainly plotted in two regions, first in the linear region where the graph shows a sharp decrease and then in the non-linear region where the graph shows saturation behaviour at very low strain amplitude; the viscoelastic modulus is independent of the applied strain. This region is known as the Linear Viscoelastic region (LVE). In LVE region,  $G'$  is higher than the  $G''$ . The magnetic force in this area dominates the hydrodynamic force, and the applied shear stress is unable to break the structures formed by a magnetic field. By further increasing the strain amplitude, a point comes where  $G'=G''$ , known as the sol-gel transition point ( $\gamma_c$ ).

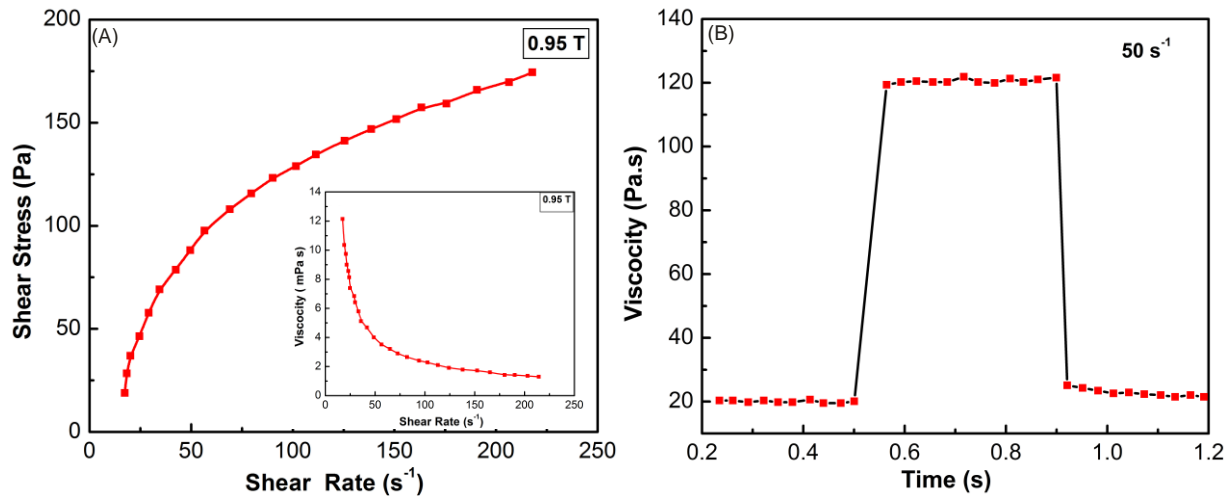


**Figure 3.** a) Shear Stress plot of the Ferrofluid as a function of shear rate at the constant applied field; inset is the Viscosity plot of the sample concerning shear rate, b) Relaxation curve showing viscosity vs time plot at a constant shear rate

At this point, the CFO FF has an equal elastic and viscous property. In addition, by increasing the strain amplitude,  $G''$  starts to dominate over  $G'$ , which implicates the dominance of the hydrodynamic force over the magnetic force. In this region, the structures break at a very high speed, decreasing the elastic property of the fluid. Above 85% of strain amplitude, all the structures break completely, and fluid becomes entirely viscous. This region is known as the saturation region,  $G'' > G'$ . The variation effect of

the angular frequency ( $0-100\omega$ ) on  $G'$  and  $G''$  is studied by frequency sweep on Ferrofluid with constant strain amplitude and magnetic field. It is evident from [Figure 4b](#) that with increasing angular frequency ( $\omega$ ),  $G'$  and  $G''$  increases, but  $G'$  increases with greater extent compared to  $G''$ . This is due to the fact that during the application of a magnetic field, structure induced by the field is formed, which ultimately increases the storage capacity of the Ferrofluid.

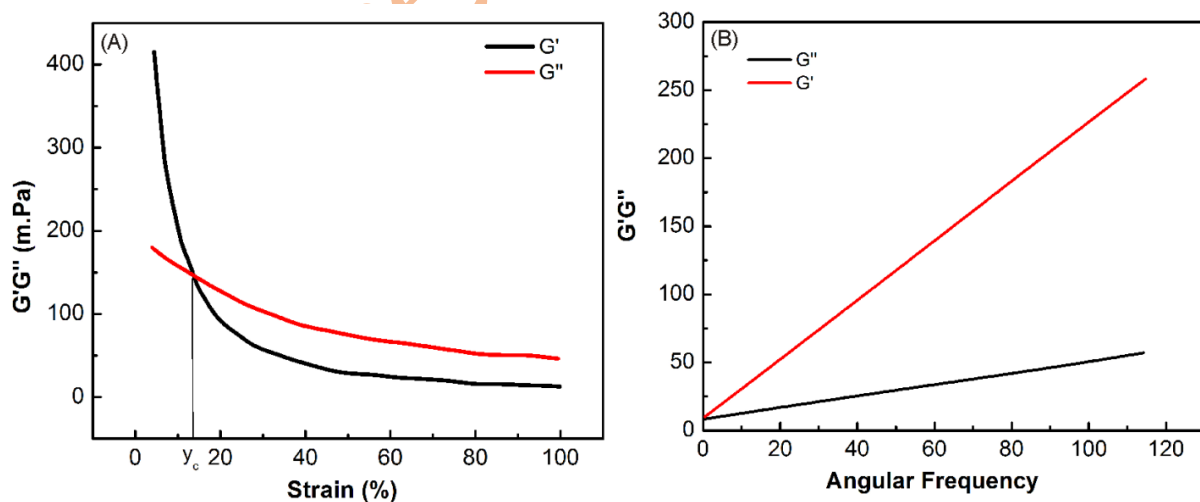


**Figure 4.** a) Effect of strain amplitude sweep on  $G'$  &  $G''$  b) Frequency sweep variation on  $G'$  &  $G''$  at constant strain and magnetic field



At very low angular frequency, the viscoelastic modulus is independent of the applied angular frequency, but at a high angular frequency, the fluid shows low time relaxation. The loss factor at a lower frequency may be greater than unity, but the loss factor is less than unity in the high-frequency region. This is why the difference between  $G'$  &  $G''$  increases as the frequency increases. The effect of viscosity on the storage modulus,  $G'$  is greater than the loss module ( $G''$ ).

## Conclusions

In this study, we discussed the synthesis and characterization of the  $\text{CoFe}_2\text{O}_4$  ferrofluid. The ferrofluids are synthesized by the green modified co-precipitation method using *G. glabra* as a surfactant. There is no literature data on the synthesis of CFO FF using *G. glabra* root extracts as a surfactant to the best of our knowledge. We also discussed various characterization techniques such as XRD for structural characterization, HRTEM for morphology, and VSM for magnetic measurements. The XRD and W-H plot confirms the purity of the CFO FF spinel structure and average crystallite size ( $D = \sim 5$  nm), strain ( $\epsilon = \sim 0.01$ ) and lattice constant ( $a = 8.39 \text{ \AA}$ ). FTIR result indicated that the sample was spinel cobalt ferrite at a wavenumber of around  $574 \text{ cm}^{-1}$ . The TEM analysis showed that the green modified co-precipitation method using *G. glabra* has led to the well-dispersed and spherical shape with an average particle size of around 12.6 nm. The magnetic measurements show that the ferromagnetic nature of the sample with saturation magnetization is  $56.6 \text{ emu/g}$ . The as-synthesized Ferrofluid essentially behaved as non-Newtonian fluids under the magnetic field; the shear stress/viscosity increased due to the formation of string-like clusters of nanoparticles oriented in the field direction. The frequency sweep concludes the increment of the elastic modulus

on the increase in the frequency due to the increase in dipolar interaction. In addition, the relaxation curve shows the time-dependent viscosity during the application and removal of the magnetic field. Moreover, time is an important factor in the development and destruction of agglomerated structures. The relaxation mechanism with size variation gives an overview of the stability of ferrofluids. As per the above results, the green modified co-precipitation synthesis found to be an effective method to obtain CFO FF, which can be used for various medical applications.

## Acknowledgements

The authors declare no acknowledgments.

## Disclosure Statement

No potential conflict of interest was reported by the authors.

## Orcid

Meet A. Moradiya  0000-0002-9012-9064

Pradeep Kumar Khiriya  0000-0003-0347-7149

## References

- [1]. Pillai V., Shah D.O. *J. Magn. Magn. Mater.*, 1996, **163**:243
- [2]. Zain N.M., Shafi A.A. *J. Adv. Res. Mater. Sci.*, 2016, **26**:1
- [3]. Fried T., Shemer G., Markovich G. *Adv. Mater.*, 2001, **13**:1158
- [4]. Sheikholeslami M., Shehzad S.A. *Int. J. Heat Mass Transf.*, 2017, **109**:82
- [5]. Zakinyan A.R., Dikansky Y.I. *J. Magn. Magn. Mater.*, 2017, **431**:103
- [6]. Yang C., Yu M., Zhao S., Tian Y., Bian X. *Nanoscale Res. Lett.*, 2018, **13**:1

- [7]. Özbey A., Karimzadehkhoei M., Yalçın S.E., Gozuacik D., Koşar A. *Microfluid.Nanofluidics*, 2015, **18**:447
- [8]. Pala J., Mehta H., Mandaliya R., Moradiya M., Savaliya C.R., Markna J.H. *MOJ Biol. Med.*, 2017, **2**:174
- [9]. Moradiya M.A., Ladani A., Ladani J., Raiyani Markna J.H. *J ChemSci Eng.*, 2017, **2**:58
- [10]. Nakatsuka K., Jeyadevan B., Neveu S., Koganezawa H. *J. Magn. Magn. Mater.*, 2002, **252**:360
- [11]. Song J., Wang L., Xu N., Zhang Q. *J. Rare Earths.*, 2010, **28**:451
- [12]. Homa D., Pickrell G. 2014, **14**:3891
- [13]. Naseri M.G., Saion E.B., Ahangar H.A., Shaari A.H., Hashim M. *Journal of Nanomaterials*, 2010, 2010:8 paages
- [14]. [Anastas P.T., Warner J.C. Oxford University Press, 1998](#)
- [15]. Ezzatzadeh E. *De Gruyter*, 2018, **73(3-4)**:179
- [16]. Ezzatzadeh E., Sofla S.F.I., Pourghasem E., Rustaiyan A., Zarezadeh Z. *J. Essent. Oil-Bear. Plants.*, 2014, **17**:415
- [17]. Fardood S.T., Moradnia F., Ghalaichi A.H., Daneshpajoo Sh., Heidari M. *NanochemRes.*, 2020, **5**:69
- [18]. Bhanvase B., Pawade V., Dhoble S.J., S. Sonawane S., Muthupandian A. *Elsevier*, 2018
- [19]. Fardood S.T., Ramazani A., Golfar Z., Joo S.W. *J. Appl. Chem. Res.*, 2017, **11**:19
- [20]. Fardood S.T., Moradnia F., Moradi S., Forootan R., Yekke Z.F., Heidari M. *Nanochem Res.*, 2019, **4**:140
- [21]. Fardood S.T., Moradnia F., Mostafaei M., Afshari Z., Faramarzi V., Ganjkhanlu S. *Nanochem Res.*, 2019, **4**:86
- [22]. Amini I., Azizkhani V., Ezzatzadeh E., Pal K., Rezayati S., Fekri M.H., Shirkhani P. *Asian J. Green Chem.*, 2020, **4**:51
- [23]. Ezzatzadeh E., Hossaini Z. *Nat. Prod. Res.*, 2020, **34**:923
- [24]. Ezzatzadeh E., Hossaini Z., Rostamian R., Vaseghi S., Mousavi S.F. *J. Heterocyclic Chem.*, 2017
- [25]. Atrak K., Ramazani A., Fardood S.T. *Environ. Technol.*, 2020, **41**:2760
- [26]. Moradnia F., Fardood S.T., Ramazani A., Osali S., Abdolmaleki I. *Micro Nano Lett.*, 2020, **15**:674
- [27]. Moradniaa F., Fardood S.T., Ramazani A., Minc B., WooJood S., Varma R.S. *J. Cleaner Prod.*, 2021, **288**:125632
- [28]. Ahankara H., Fardood S.T., Ramazanib A. *Iran. J. Catal.*, 2020, **10**:195
- [29]. Ezzatzadeh E., Hossaini Z., Moradi A.V., Salimifard M., Sharif Abad S.A. *Can. J. Chem.*, 2019, **97**:270
- [30]. Amini I., Azizkhani V., Ezzatzadeh Z., Pal K., Rezayati S., Fekri M.H., Shirkhani P. *Asian J. Green Chem.*, 2020, **4**:51
- [31]. Mansour S.S., Ezzatzadeh E., Safarkar R. *Asian J. Green Chem.*, 2019, **3**:353
- [32]. Jivani A., Moradiya M.A. *J. Sci. Technol.*, 2020, **5**:213
- [33]. Moradiya M.A., Dangodara A., Pala J., Savaliya C.R., Dhruv D., Rathod V.R., Joshi A.D., Shah N.A., Pandya D., Markna J.H. *Sep. Sci. Technol.*, 2019, **54**:207
- [34]. Shaikh R., Syed I.Z., Bhende P. *Asian J. Green Chem.*, 2019, **3**:70
- [35]. Manikandan M., Durka S., Antony A. *J. Inorg. Organomet. Polym.*, 2015, **25**:1019
- [36]. Gingașu D., Mîndru I., preda S., calderon-moreno J.M., culiță L. patrona D.C., diamandescub L. *Rev. Roum. Chim.*, 2017, **62**:645
- [37]. Kombaiah K., Vijaya J.J., Kennedy L.J., Bououdina M., Ramalingam R.J., Al-Lohedan H.A. *Mater. Chem. Phys.*, 2018, **204**:410
- [38]. Anburaj R., Jothi prakasam V., Nadu T. *International Journal of Pharmaceutical Sciences Review and Research*, 2018, **51**:137
- [39]. Shahmiria N., Manteghi F., Sohrabia B., Golafshanb S., *The 18<sup>th</sup> International Electronic*

*Conference on Synthetic Organic Chemistry*, 2013, **31**:924

[40]. Al-snafi A.E. *IOSR J. Pharm.*, 2018, **8**:1

[41]. Kalsi S., Verma S.K., Kaur A., Singh N. *Int. J. Pharm. Drug Anal.*, 2016, **4**:234

[42]. Lawrence K., Pawan K., Amarendra N., Manoranjan K. *Int. Nano Let.*, 2013, **8**:1

[43]. El-Okr M.M., Salem M.A., Salim M.S., El-Okr R.M., Ashoush M., Talaat H.M. *J. Magn. Magn. Mater.*, 2011, **323**:920

[44]. Radhika B., Sahoo R., Srinath S. *AIP Conf. Proc.*, 2015, **1665**:1

[45]. Hong R.Y., Ren Z.Q., Han Y.P., Li H.Z., Zheng Y., Ding J. *Chem. Eng. Sci.*, 2007, **6**:5912

[46]. Ghasemi E., Mirhabibi A., Edrissi M. *J. Magn. Magn. Mater.*, 2008, **320**:2635

[47]. Yang C., Yu M., Zhao S., Tian Y., Bian X. *Nanoscale Res. Lett.*, 2018, **13**:378

**How to cite this manuscript:** Meet A. Moradiya, Pradeep Kumar Khiriya, Purnima Swarup Khare. Green synthesis of  $\text{CoFe}_2\text{O}_4$  ferrofluid: Investigation of structural, magnetic and rheological behaviour. *Asian Journal of Nanoscience and Materials*, x(x) 2021, xx-xx. DOI: 10.26655/AJNANOMAT.2021.3.9